JOURNAL OF COMPUTATIONAL PHYSICS **124,** 217–229 (1996)
ARTICLE NO. 0054

Iterative Implementation of an Implicit–Explicit Hybrid Scheme for Hydrodynamics

WENLONG DAI AND PAUL R. WOODWARD

University of Minnesota, 1100 Washington Avenue South, 101, Minneapolis, Minnesota 55415

Received November 28, 1994; revised May 1, 1995

Iterative implementation of an implicit—explicit hybrid scheme for solving the Euler equations is described in this paper. The scheme was proposed by Fryxell *et al.* (*J. Comput. Phys.* **63,** 283 (1986)), is of the Godunov-type in both explicit and implicit regimes, is conservative, and is accurate to second order in both space and time for all Courant numbers. Only a single level of iterations is involved in the implementation, which solves both the implicit relations arising from upstream centered differences for all wave families and the nonlinearity of the Euler equations. The number of iterations required to reach a converged solution may be significantly reduced by the introduction of the multicolors proposed in this paper. Only a small number of iterations are needed in the scheme for a simulation with large time steps. The multicolors may also be applied to other linear and nonlinear wave equations for numerical solutions.

1. INTRODUCTION

During the last 20 years, Godunov schemes for hydrodynamics have been developed, which have been particularly efficient for shock problems. Godunov [1] supposed that the initial data could be replaced by a set of piecewise constant data with discontinuities and used exact solutions of Riemann problems to advance the piecewise constant data. A major extension to the Godunov's scheme was made by Van Leer in his MUSCL scheme [2, 3] which used a Riemann solver to advance piecewise linear data. Other examples of Godunov schemes include Roe's method [4], the piecewise parabolic method (PPM) [5, 6], the TVD method [7]. One of the key points in Godunov schemes is to calculate the flux at each interface of numerical cells through a Riemann problem.

Godunov schemes for hydrodynamical equations may be second-order accurate in time, but they are explicit. The time step in an explicit scheme is restricted by the largest Courant number, which cannot be larger than unity for a stable calculation. The stability limit in an explicit scheme is imposed by the local conditions in the regions, where wave speeds are high, regardless of the significance of spatial variations prevailing in the problems. The regions drastically reduce the time step possible from explicit schemes. Implicit schemes for hydrodynamical equations are favored over their explicit counterparts for some problems, in which the time-step size necessary for procuring a required temporal accuracy may be significantly larger than that dictated by the explicit stability condition. Implicit–explicit hybrid schemes are useful when a flow attains different wave speeds either in different regions or at different instants, and the time accuracy is important in some parts of simulation domains.

Implicit and implicit–explicit hybrid schemes for hydrodynamical equations have been developed for many years. Schemes with a smooth switch for advection have been in use for many years (for example, see [8, 9]). Beam and Warming [10] proposed an implicit scheme for hyperbolic systems of conservation laws. Engquist and Osher [11] proposed a method for transonic flows. Van Leer and Mulder [12] developed a scheme which is time-accurate for small time steps and turns into a relaxation method for large time steps. Yee *et al.* [13] proposed an implicit TVD scheme for steady states. Glaz and Wardlaw [14] proposed a high-order Godunov scheme for steady supersonic gas dynamics. Fryxell *et al.* [15] developed a method which extends Godunov schemes to the implicit regime. Jameson and Yoon [16, 17] proposed an implicit scheme which is combined with the multigrid method. More recently, Loh and Hui [18] developed a first-order Godunov scheme for steady supersonic flows; Blunt and Rubin [19] extended a TVD scheme to fully implicit and partially implicit regimes; Wilcoxson and Manousiouthankis [20] developed implicit time marching implementation of the essentially nonoscillatory scheme.

A typical approach in implicit schemes is linearization which results in a linear system. The linear system is then exactly or approximately solved. The Newton iteration is often used in implicit schemes. But, the Newton iteration in an implicit scheme is very time-consuming. An exact linear solver in an implicit scheme is difficult to vectorize and needs large memory. Therefore, iterative linear solvers are often used for the linear system. But an iterative approach often needs a large number of iterations. The work to be presented here is based on the framework reported in [15]. In this paper, we propose an iterative approach. The

0021-9991/96 $18.00

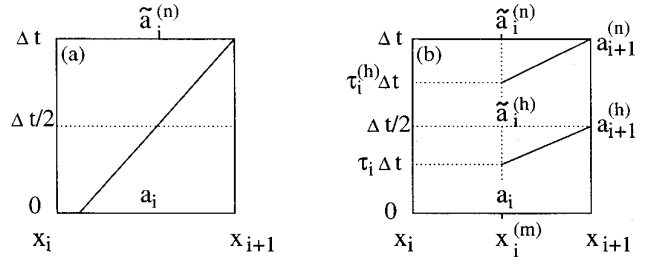

FIG. 1. The structure of a cell in space–time for two kinds of situations, one with the Courant number less than unity (a) and the other with the number greater than unity (b). In the first case, the time-average of $a(x, t)$ over the time step Δt at x_{i+1} is equal to the cell-average of a over the domain $[x_{i+1} - c\Delta t, x_{i+1}]$ at $t = 0$. In the other case, an extra time level at $t = \Delta t/2$ is introduced, and two characteristic curves passing through $(x_{i+1}, \Delta t/2)$ or $(x_{i+1}, \Delta t)$ are traced back to the center $x_i^{(m)}$ of the cell.

iterative approach involves only a single level of iterations, which solve both the implicit relations arising from upstream centered differences for all wave families and the nonlinearity of the Euler equations. Only a small number of iterations are needed in the scheme for a simulation with large time steps. This paper deals with only the one-dimensional situation, and is the first step to develop a hybrid scheme for the multi-dimensional Euler equations.

The plan of this paper is as follows. The second section is an illustration of the iterative implementation through linear advection. The iterative implementation of the scheme for the Euler equations is in the third section. The numerical examples are in the forth section, and the final section is for the conclusions and a brief discussion.

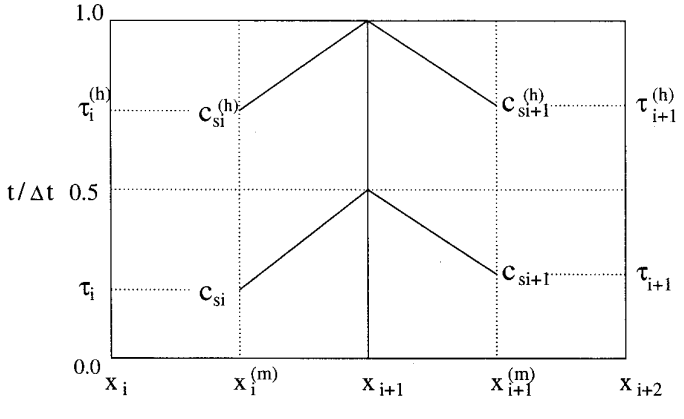

FIG. 2. An illustration for the calculation of the interface values at $x = x_{i+1}$ in the case with Courant numbers larger than unity. Two characteristic curves pass through the point $(x_{i+1}, \Delta t/2)$, and other two pass through the point $(x_{i+1}, \Delta t)$. $x_i^{(m)}$ and $x_{i+1}^{(m)}$ are the centers of the two cells near the interface. The interface values at x_{i+1} and at $t = \Delta t/2$ and Δt may be obtained through two Riemann problems, and may be written in terms of cell-averages. A cell-average of any variable at $t \in [0, \Delta t]$ may be obtained through parabolic interpolation in time, and a parabola is uniquely determined by cell-averages at $t = 0$, $\Delta t/2$ and Δt.

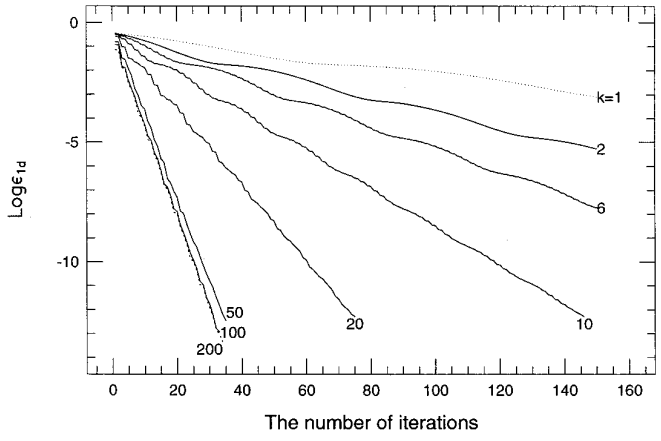

FIG. 3. The convergence when 200 numerical cells and a time step 0.2 are used. Courant numbers are around 40. The wave travels about one-fifth of its wavelength during the time step. The dotted lines indicated by $k = 1$ results from the approach $\mathbf{A}_1$, the solid lines are obtained from the approach $\mathbf{A}_k$ for $k = 2$, 6, 10, 20, 50, and 100, and the dashed line comes from the approach $\mathbf{A}_N$. The initial condition and the wave after it travels one time step are shown in Fig. 8.

2. A LINEAR ADVECTION SCHEME

We first illustrate the iterative implementation for linear advection

$$\frac{\partial a}{\partial t} + c\frac{\partial a}{\partial x} = 0, \tag{1}$$

where x and t are the space and time coordinates, a is the quantity being advected, and c is a constant advection

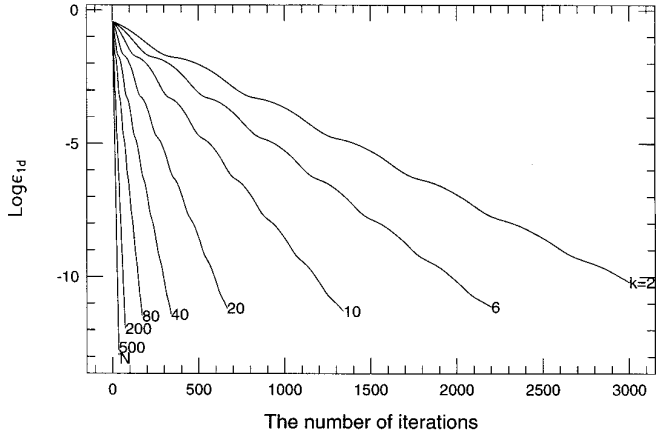

FIG. 4. The convergence when 2000 numerical cells and a time step 0.2 are used. Courant numbers are around 400. The wave travels about one-fifth of its wavelength during the time step. The solid lines are obtained from the approach $\mathbf{A}_k$ for $k = 6$, 10, 20, 40, 80, 200, and 500, and the dashed line comes from the approach $\mathbf{A}_N$.

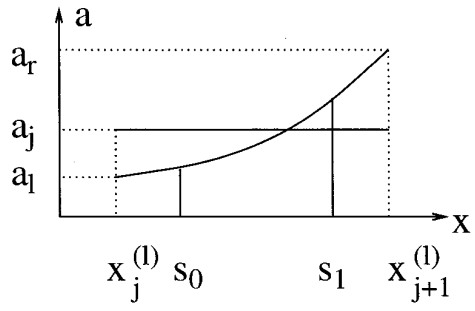

FIG. 5. An illustration for the calculation of a conserved quantity a in a part $[s_0, s_1]$ of a cell $[x_j^{(l)}, x_{j+1}^{(l)}]$.

velocity. Considering a numerical cell $[x_i, x_{i+1}]$, we write Eq. (1) in a difference form:

$$\tilde{a}_i^{(n)} = a_i - \frac{c\Delta t}{\Delta x_i}(\bar{a}_{i+1} - \bar{a}_i). \tag{2}$$

Here Δx_i is the width of the cell, Δt is the time step, $\tilde{a}_i^{(n)}$ (or a_i) is the cell-average of a over the cell at $t = \Delta t$ (or $t = 0$), and $\bar{a}_i$ is the time-average of a at x_i over the time step, i.e.,

$$\tilde{a}_i^{(n)} \equiv \frac{1}{\Delta x_i}\int_{x_i}^{x_{i+1}} a(x, \Delta t)\, dx,$$

$$\bar{a}_i \equiv \frac{1}{\Delta t}\int_0^{\Delta t} a(x_i, t)\, dt.$$

For the case in which the Courant number σ_i ($\equiv c\Delta t/\Delta x_i$) is less than unity (Fig. 1a), the time-average $\bar{a}_{i+1}$ is equal to the domain-average of a over the domain of dependence $[x_{i+1} - c\Delta t, x_{i+1}]$, and the scheme is unconditionally stable.

For the case in which the Courant number is greater than unity, the domain of dependence extends beyond a cell interface, and thus the time-average $\bar{a}_{i+1}$ cannot be calculated from the distribution of a over the neighbor cell. In this case, Fryxell *et al.* [15] introduced an extra time level at $t = \Delta t/2$ (Fig. 1b).

For the first half time step, we have an equation similar to Eq. (2):

$$\tilde{a}_i^{(h)} = a_i - \frac{c\Delta t}{2\Delta x_i}(\bar{a}_{i+1}^{(h)} - \bar{a}_i^{(h)}). \tag{3}$$

Here $\tilde{a}_i^{(h)}$ is the cell-average of a at $t = \Delta t/2$, and $\bar{a}_i^{(h)}$ is the time-average of a over the first half time step at $x = x_i$. The time-averages, $\bar{a}_i$ and $\bar{a}_i^{(h)}$, may be approximately calculated through a linear interpolation in time. The linear interpolation in uniquely determined by $a_i^{(h)}$ ($\equiv a(x_i, \Delta t/2)$) and $a_i^{(n)}$ ($\equiv a(x_i, \Delta t)$). Thus, Eqs. (2), (3) may be written as

$$\tilde{a}_i^{(n)} = a_i - \sigma_i(a_{i+1}^{(h)} - a_i^{(h)}), \tag{4}$$

$$\tilde{a}_i^{(h)} = a_i - \tfrac{1}{2}\sigma_i[\tfrac{3}{2}a_{i+1}^{(h)} - \tfrac{1}{2}a_{i+1}^{(n)} - (\tfrac{3}{2}a_i^{(h)} - \tfrac{1}{2}a_i^{(n)})]. \tag{5}$$

In order to find $a_{i+1}^{(n)}$ and $a_{i+1}^{(h)}$, two characteristic curves passing through $(x_{i+1}, \Delta t)$ or $(x_{i+1}, \Delta t/2)$ in the $(x - t)$-space are traced back to the center of the cell, $x_i^{(m)} \equiv (x_{i+1} + x_i)/2$ (see Fig. 1b). $a_{i+1}^{(n)}$ and $a_{i+1}^{(h)}$ are equal to $a(x_i^{(m)}, \tau_i^{(h)}\Delta t)$ and $a(x_i^{(m)}, \tau_i\,\Delta t)$, respectively. Here $\tau_i^{(h)}$ and τ_i are defined as

$$\tau_i^{(h)} \equiv 1 - \frac{1}{2\sigma_i}, \quad \tau_i \equiv \frac{1}{2}\left(1 - \frac{1}{\sigma_i}\right). \tag{6}$$

Up to second order of accuracy, $a(x_i^{(m)}, \tau_i^{(h)}\Delta t)$ and $a(x_i^{(m)}, \tau_i\,\Delta t)$ are the cell-averages of a over the cell $[x_i, x_{i+1}]$ at $t = \tau_i^{(h)}\Delta t$ and $t = \tau_i\,\Delta t$, respectively, which may be approximately calculated through a parabolic interpolation for the cell-average $\tilde{a}_i(t)$ in the time. The parabola is uniquely determined by three cell-averages, a_i, $\tilde{a}_i^{(h)}$, and $\tilde{a}_i^{(n)}$. Therefore $a_{i+1}^{(n)}$ and $a_{i+1}^{(h)}$ may be written as

$$a_{i+1}^{(n)} = a_i + (-\delta a_i^{(n)} + 4\delta a_i^{(h)})\tau_i^{(h)} + (2\delta a_i^{(n)} - 4\delta a_i^{(h)})(\tau_i^{(h)})^2, \tag{7}$$

$$a_{i+1}^{(h)} = a_i + (-\delta a_i^{(n)} + 4\delta a_i^{(h)})\tau_i + (2\delta a_i^{(n)} - 4\delta a_i^{(h)})\tau_i^2. \tag{8}$$

Here $\delta a_i^{(n)}$ and $\delta a_i^{(h)}$ are defined as

$$\delta a_i^{(n)} \equiv \tilde{a}_i^{(n)} - a_i,$$

$$\delta a_i^{(h)} \equiv \tilde{a}_i^{(h)} - a_i.$$

If interface values $a_i^{(n)}$ and $a_i^{(h)}$ in Eqs. (4), (5) are eliminated through Eqs. (7), (8), we will have a block-bidiagonal system of linear equations which can be solved for $\tilde{a}_i^{(n)}$ and $\tilde{a}_i^{(h)}$. It has been shown [15] that the scheme is unconditionally stable for Courant numbers greater than unity.

Our purpose is to find an iterative approach for cell-averages $\tilde{a}_i^{(n)}$ ($i = 1, 2, ...$). From an initial guess for interface values $a_i^{(n)}$ and $a_i^{(h)}$, a straightforward procedure is to calculate cell-averages, $\tilde{a}_i^{(n)}$ and $\tilde{a}_i^{(h)}$, through Eqs. (4), (5) followed by an improvement of the interface values through Eqs. (7), (8). Unfortunately, numerical experiments show that this iterative procedure does not converge when the Courant number is larger than unity. This is because that the error in $\tilde{a}_i^{(n)}$ is increased by a factor of the Courant number through each iteration for Eq. (3).

Our approach for the linear advection is as follows: We

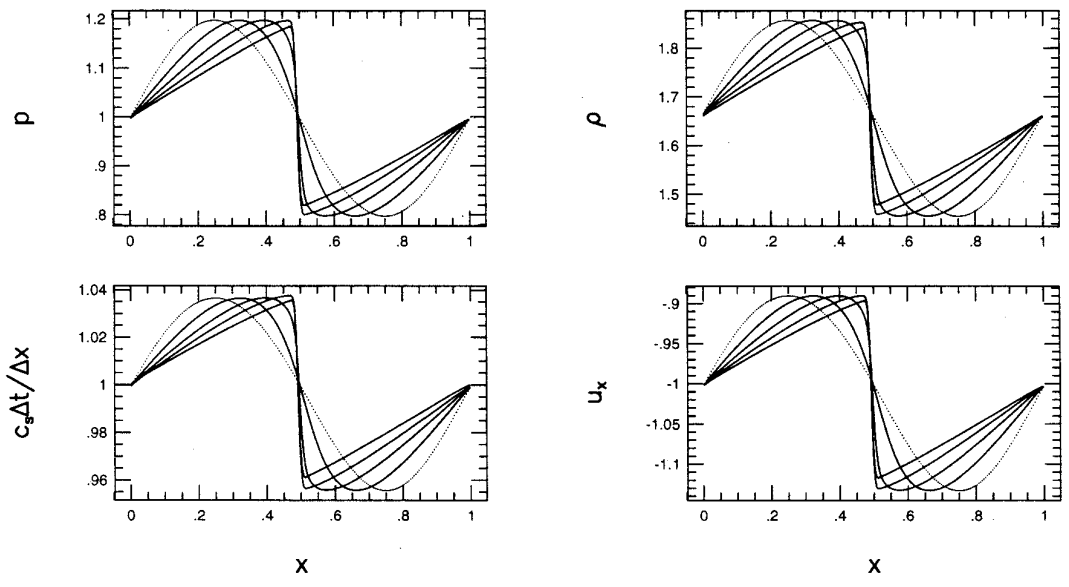

FIG. 6. The propagation of a sound wave: 200 cells in [0, 1]; $\Delta t = 0.005$; 2 iterations. Dotted lines are initial profiles, and solid lines are the profiles at $t = 0.5$, 1.0, 1.5, and 2.0. The results show a smooth switch between explicit and implicit calculations.

eliminate $\tilde{a}_{i+1}^{(n)}$ and $\tilde{a}_{i+1}^{(h)}$ in Eqs. (4), (5) through Eqs. (7), (8) to obtain

$$(1 + \sigma_i\alpha_i^{(h)})\delta a_i^{(n)} + \sigma_i\beta_i^{(h)}\delta a_i^{(h)} = \sigma_i(\alpha_i^{(h)} - a_i), \tag{9}$$

$$\tfrac{1}{4}\sigma_i(3\alpha_i^{(h)} - \alpha_i^{(n)})\delta a_i^{(n)} + [1 + \tfrac{1}{4}\sigma_i(3\beta_i^{(h)} - \beta_i^{(n)})]\delta a_i^{(h)} = \tfrac{1}{4}\sigma_i(3a_i^{(h)} - a_i^{(n)}) - \tfrac{1}{2}\sigma_i a_i. \tag{10}$$

Here $\alpha_i^{(n)}, \beta_i^{(n)}, \alpha_i^{(h)}$, and $\beta_i^{(h)}$ are defined as

$$\alpha_i^{(n)} \equiv \tau_i^{(h)}(2\tau_i^{(h)} - 1), \quad \beta_i^{(n)} \equiv 4\tau_i^{(h)}(1 - \tau_i^{(h)}), \tag{11}$$

$$\alpha_i^{(h)} \equiv \tau_i(2\tau_i - 1), \quad \beta_i^{(h)} \equiv 4\tau_i(1 - \tau_i). \tag{12}$$

We initially guess interface values, $a_i^{(n)}$ and $a_i^{(h)}$, and then calculate cell-averages $\tilde{a}_i^{(n)}$ and $\tilde{a}_i^{(h)}$ through solving Eqs. (9), (10) for $\delta a_i^{(n)}$ and $\delta a_i^{(h)}$. The interface values are improved through Eqs. (7), (8) with the right hand side (RHS) of Eqs. (7), (8) evaluated at the improved cell-averages.

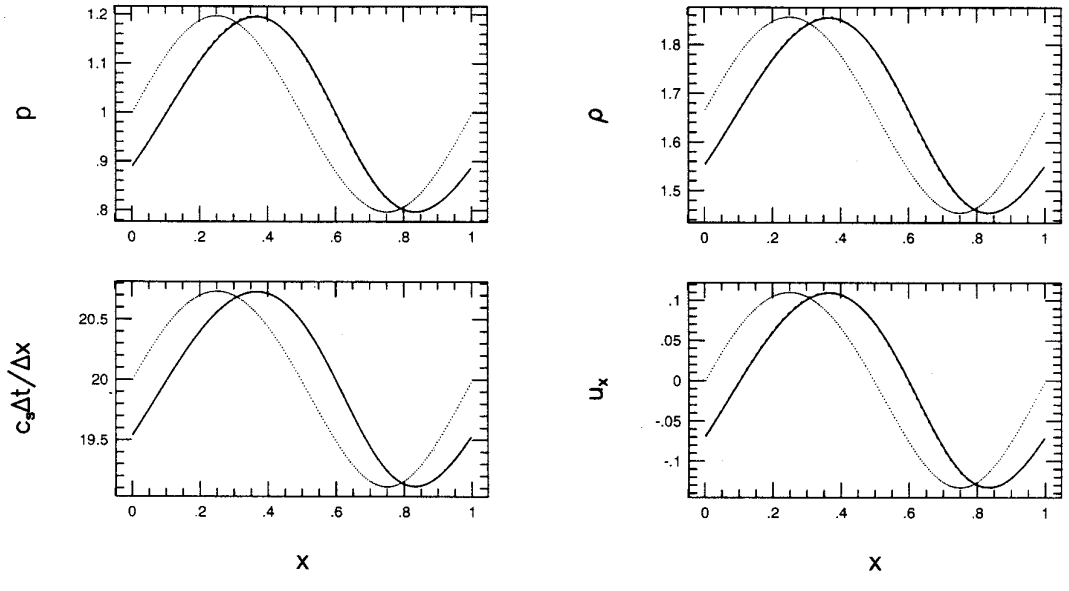

FIG. 7. The sound wave (solid lines) after one time step $\Delta t = 0.1$; 200 cells in [0, 1]; 6 iterations. The initial condition is shown by dotted lines. Dashed lines are from an explicit scheme, which are overlapped by solid lines.

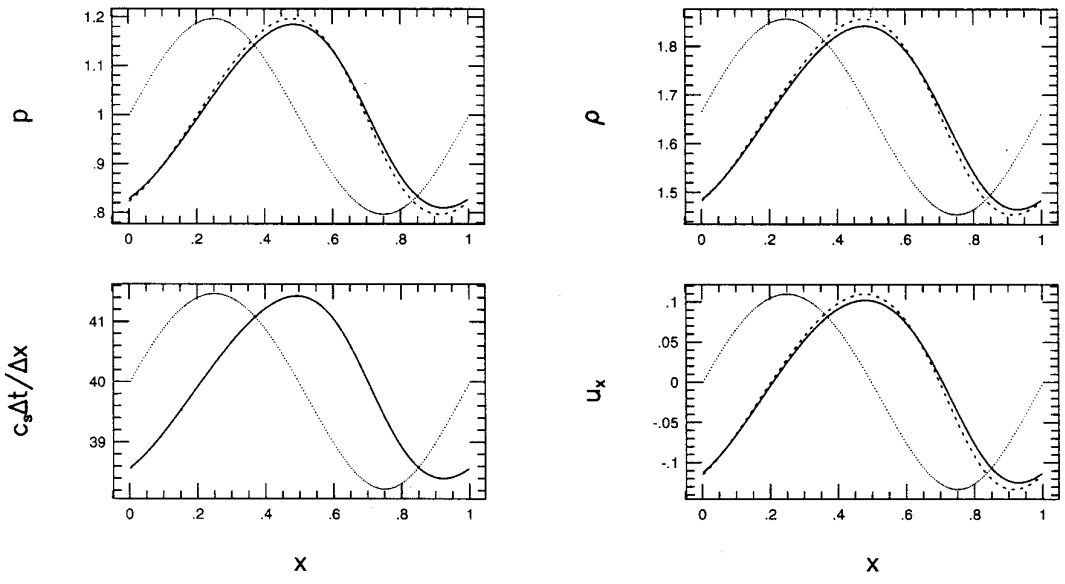

FIG. 8. The sound wave (solid lines) after one time step $\Delta t = 0.2$; 200 cells in [0, 1]; 10 iterations. The initial condition is shown by the dotted lines. Dashed lines are from an explicit scheme.

One iteration consists of the two sets of calculations, one for Eqs. (9), (10) and the other for Eqs. (7), (8). The next iteration may be started from the improved interface values. Numerical experiments show that this iterative procedure converges. We will show the convergence in the next section.

3. A SCHEME FOR HYDRODYNAMICS

The iterative procedure described in the last section can be extended for use in the Euler equations. In this paper, we consider only the one-dimensional situation. We also limit the discussion to the γ-law for the equation of state, although a more general equation of state can be accommodated. The Euler equations are

$$\frac{\partial \rho}{\partial t} + \frac{\partial}{\partial x}(\rho u) = 0, \tag{13}$$

$$\frac{\partial}{\partial t}(\rho u) + \frac{\partial}{\partial x}(\rho u^2 + p) = 0, \tag{14}$$

$$\frac{\partial}{\partial t}(\rho E) + \frac{\partial}{\partial x}[u(\rho E + p)] = 0. \tag{15}$$

Here ρ is the mass density, u is the flow velocity, p is the pressure, E is the total specific energy defined as $E \equiv e + u^2/2$ with e being the specific internal energy. The pressure is related to the internal energy through the γ-law $p = (\gamma - 1)\rho e$ with γ being the ratio of the specific heat capacities.

We implement a dynamical step in a Lagrangian coordinate followed by an explicit mapping at the end of each dynamical step. Therefore we write the Euler equations in a Lagrangian form:

$$\frac{\partial V}{\partial t} = \frac{\partial u}{\partial m}, \tag{16}$$

$$\frac{\partial u}{\partial t} = -\frac{\partial p}{\partial m}, \tag{17}$$

$$\frac{\partial E}{\partial t} = -\frac{\partial uP}{\partial m}, \tag{18}$$

where V is the specific volume ($\equiv 1/\rho$), and m is the mass coordinate defined as $dm \equiv \rho\, dx$.

The differentials of Riemann invariants for two sound waves have the form

$$dR_{\pm} \equiv dp \pm C_s\, du. \tag{19}$$

Here the plus (or minus) sign is for the wave propagating in the positive (or negative) x-direction, and C_s is the sound speed in the mass coordinate. The sound speed in the space coordinate, c_s, may be obtained through dividing C_s by the mass density ρ.

Consider a numerical grid $\{x_i\}$ and its corresponding grid in the mass coordinate $\{m_i\}$. Integrating Eqs. (16)–(18) in a rectangular $m_i \le m \le m_{i+1}$ and $0 \le t \le \Delta t$, we have difference equations:

$$\tilde{V}_i^{(n)} = V_i + \frac{\Delta t}{\Delta m_i}(\overline{u}_{i+1} - \overline{u}_i),$$

$$\tilde{u}_i^{(n)} = u_i - \frac{\Delta t}{\Delta m_i}(\overline{p}_{i+1} - \overline{p}_i),$$

$$\tilde{E}_i^{(n)} = E_i - \frac{\Delta t}{\Delta m_i}[(\overline{pu})_{i+1} - (\overline{pu})_i].$$

Here Δm_i is the mass contained in the cell $[x_i, x_{i+1}]$.

We approximately calculate a time-average through a linear interpolation of an interface value along time. The linear interpolation is uniquely determined by interface values at $t = \Delta t/2$ and Δt. Therefore the set of difference equations above may be approximately written as

$$\tilde{V}_i^{(n)} = V_i + \frac{\Delta t}{\Delta m_i}(u_{i+1}^{(h)} - u_i^{(h)}), \tag{20}$$

$$\tilde{u}_i^{(n)} = u_i - \frac{\Delta t}{\Delta m_i}(p_{i+1}^{(h)} - p_i^{(h)}), \tag{21}$$

$$\tilde{E}_i^{(n)} = E_i - \frac{\Delta t}{\Delta m_i}(u_{i+1}^{(h)} p_{i+1}^{(h)} - u_i^{(h)} p_i^{(h)}). \tag{22}$$

Here we have treated the time-average of a product of two variables approximately as the product of two time-averages. This approximation is accurate to second order in time. Similarly, the cell-averages after a half time step may be written as

$$\tilde{V}_i^{(h)} = V_i + \frac{\Delta t}{2\,\Delta m_i}\left[\frac{3}{2}u_{i+1}^{(h)} - \frac{1}{2}u_{i+1}^{(n)} - \left(\frac{3}{2}u_i^{(h)} - \frac{1}{2}u_i^{(n)}\right)\right], \tag{23}$$

$$\tilde{u}_i^{(h)} = u_i - \frac{\Delta t}{2\,\Delta m_i}\left[\frac{3}{2}p_{i+1}^{(h)} - \frac{1}{2}p_{i+1}^{(n)} - \left(\frac{3}{2}p_i^{(h)} - \frac{1}{2}p_i^{(n)}\right)\right], \tag{24}$$

$$\tilde{E}_i^{(h)} = E_i - \frac{\Delta t}{2\,\Delta m_i}\left[\left(\frac{3}{2}u_{i+1}^{(h)} - \frac{1}{2}u_{i+1}^{(n)}\right)\left(\frac{3}{2}p_{i+1}^{(h)} - \frac{1}{2}p_{i+1}^{(n)}\right) - \left(\frac{3}{2}u_i^{(h)} - \frac{1}{2}u_i^{(n)}\right)\left(\frac{3}{2}p_i^{(h)} - \frac{1}{2}p_i^{(n)}\right)\right]. \tag{25}$$

3.1. *Iterative Approach*

Our purpose in this subsection is to develop an iterative approach to find interface values, $u_i^{(h)}$ and $p_i^{(h)}$, which are needed in Eqs. (20)–(22). For the purpose, we use a Riemann solver, which is based on the characteristic formulation, Eq. (19). Incorporating a Riemann solver does not change the structure of the iteration. As shown in Fig. 2, $u_{i+1}^{(h)}$ and $p_{i+1}^{(h)}$ may be found through two characteristic curves traced back from the point $(x_{i+1}, \Delta t/2)$ to the centers of two neighbor cells, $x_i^{(m)}$ and $x_{i+1}^{(m)}$, and, $u_{i+1}^{(n)}$ and $p_{i+1}^{(n)}$ may be found through the other set of characteristic curves traced back from the point $(x_{i+1}, \Delta t)$ to the centers. The time levels at the ends of the four characteristic curves at the centers are $\tau_i^{(h)}\Delta t$, $\tau_i\,\Delta t$, $\tau_{i+1}^{(h)}\,\Delta t$, and $\tau_{i+1}\,\Delta t$. Here

$$\tau_i^{(h)} \equiv 1 - \frac{\Delta m_i}{2C_{si}^{(h)}\,\Delta t}, \quad \tau_i \equiv \frac{1}{2}\left(1 - \frac{\Delta m_i}{C_{si}\,\Delta t}\right),$$

and C_{si} (or $C_{si}^{(h)}$) is C_s evaluated at a cell-average and at the initial time (or at $t = \Delta t/2$). For example, we may find $u_{i+1}^{(h)}$ and $p_{i+1}^{(h)}$ through solving the following set of linear equations:

$$p_{i+1}^{(h)} - p(x_i^{(m)}, \tau_i\,\Delta t) + w_{i+1}[u_{i+1}^{(h)} - u(x_i^{(m)}, \tau_i\,\Delta t)] = 0, \tag{26}$$

$$p_{i+1}^{(h)} - p(x_{i+1}^{(m)}, \tau_{i+1}\,\Delta t) - w_{i+1}[u_{i+1}^{(h)} - u(x_{i+1}^{(m)}, \tau_{i+1}\,\Delta t)] = 0. \tag{27}$$

Here $w_{i+1} \equiv (C_{si} + C_{si+1})/2$.

A cell-average of a variable, a, at any time $t \in [0, \Delta t]$ may be found through a parabola in time. The parabola is uniquely determined by the cell-averages at $t = 0$, $\Delta t/2$, and Δt. For example, $u(x_i^{(m)}, \tau_i^{(h)}\Delta t)$ and $u(x_i^{(m)}, \tau_i\,\Delta t)$ are found to be

$$u(x_i^{(m)}, \tau_i^{(h)}\,\Delta t) = u_i + (-\delta u_i^{(n)} + 4\delta u_i^{(h)})\tau_i^{(h)} + (2\delta u_i^{(n)} - 4\delta u_i^{(h)})(\tau_i^{(h)})^2, \tag{28}$$

$$u(x_i^{(m)}, \tau_i\,\Delta t) = u_i + (-\delta u_i^{(n)} + 4\delta u_i^{(h)})\tau_i + (2\,\delta u_i^{(n)} - 4\,\delta u_i^{(h)})\tau_i^2. \tag{29}$$

These two formulations are also valid for $p(x_i^{(m)}, \tau_i^{(h)}\,\Delta t)$ and $p(x_i^{(m)}, \tau_i\,\Delta t)$ if u is replaced by p.

Solving both Riemann problems and using Eqs. (28), (29), we may write interface values in terms of cell-averages:

$$\begin{aligned} u_{i+1}^{(n)} = {} & \tfrac{1}{2}[u_{i+1} + u_i - (p_{i+1} - p_i)/w_{i+1}^{(h)}] \\ & + \tfrac{1}{2}[\alpha_{i+1}^{(n)}\,\delta u_{i+1}^{(n)} + \beta_{i+1}^{(n)}\,\delta u_{i+1}^{(h)} - (\alpha_{i+1}^{(n)}\,\delta p_{i+1}^{(n)} \\ & + \beta_{i+1}^{(n)}\,\delta p_{i+1}^{(h)})/w_{i+1}^{(h)}] \\ & + \tfrac{1}{2}[\alpha_i^{(n)}\,\delta u_i^{(n)} + \beta_i^{(n)}\,\delta u_i^{(h)} + (\alpha_i^{(n)}\,\delta p_i^{(n)} \\ & + \beta_i^{(n)}\,\delta p_i^{(h)})/w_{i+1}^{(h)}], \end{aligned} \tag{30}$$

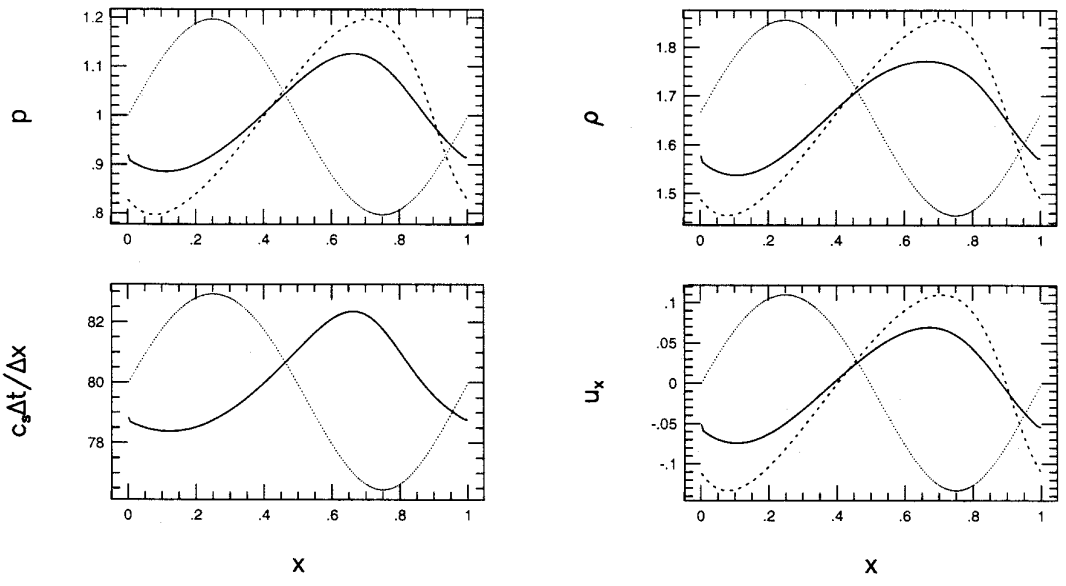

FIG. 9. The sound wave (solid lines) after one time step $\Delta t = 0.4$; 200 cells in [0, 1]; 14 iterations. The initial condition is shown by dotted lines. Dashed lines are from an explicit scheme.

$$
\begin{aligned}
p_{i+1}^{(n)} &= \tfrac{1}{2}[p_{i+1} + p_i - w_{i+1}^{(h)}(u_{i+1} - u_i)] \\
&\quad + \tfrac{1}{2}[\alpha_{i+1}^{(n)}\,\delta p_{i+1}^{(n)} + \beta_{i+1}^{(n)}\,\delta p_{i+1}^{(h)} - w_{i+1}^{(h)}(\alpha_{i+1}^{(n)}\,\delta u_{i+1}^{(n)} \\
&\quad + \beta_{i+1}^{(n)}\,\delta u_{i+1}^{(h)})] \\
&\quad + \tfrac{1}{2}[\alpha_i^{(n)}\,\delta p_i^{(n)} + \beta_i^{(n)}\,\delta p_i^{(h)} + w_{i+1}^{(h)}(\alpha_i^{(n)}\,\delta u_i^{(n)} \\
&\quad + \beta_i^{(n)}\,\delta u_i^{(h)})], \qquad (31) \\
u_{i+1}^{(h)} &= \tfrac{1}{2}[u_{i+1} + u_i - (p_{i+1} - p_i)/w_{i+1}] \\
&\quad + \tfrac{1}{2}[\alpha_{i+1}^{(h)}\,\delta u_{i+1}^{(n)} + \beta_{i+1}^{(h)}\,\delta u_{i+1}^{(h)} - (\alpha_{i+1}^{(h)}\,\delta p_{i+1}^{(n)} \\
&\quad + \beta_{i+1}^{(h)}\,\delta p_{i+1}^{(h)})/w_{i+1}] \\
&\quad + \tfrac{1}{2}[\alpha_i^{(h)}\,\delta u_i^{(n)} + \beta_i^{(h)}\,\delta u_i^{(h)} \\
&\quad + (\alpha_i^{(h)}\,\delta p_i^{(n)} + \beta_i^{(h)}\,\delta p_i^{(h)})/w_{i+1}], \qquad (32) \\
p_{i+1}^{(h)} &= \tfrac{1}{2}[p_{i+1} + p_i - w_{i+1}(u_{i+1} - u_i)] \\
&\quad + \tfrac{1}{2}[\alpha_{i+1}^{(h)}\,\delta p_{i+1}^{(n)} + \beta_{i+1}^{(h)}\,\delta p_{i+1}^{(h)} - w_{i+1}(\alpha_{i+1}^{(h)}\,\delta u_{i+1}^{(n)} \\
&\quad + \beta_{i+1}^{(h)}\,\delta u_{i+1}^{(h)})] \\
&\quad + \tfrac{1}{2}[\alpha_i^{(h)}\,\delta p_i^{(n)} + \beta_i^{(h)}\,\delta p_i^{(h)} + w_{i+1}(\alpha_i^{(h)}\,\delta u_i^{(n)} \\
&\quad + \beta_i^{(h)}\,\delta u_i^{(h)})]. \qquad (33)
\end{aligned}
$$

Here $\alpha_i^{(n)}, \beta_i^{(n)}, \alpha_i^{(h)}$, and $\beta_i^{(h)}$ are defined in Eqs. (11), (12) in terms of $\tau_i^{(h)}$ and τ_i, and $w_i^{(h)} = (C_{si}^{(h)} + \mathbf{C}_{si+1}^{(h)})/2$.

We substitute Eqs. (30)–(33) into Eqs. (20)–(25) for $u_{i+1}^{(n)}, p_{i+1}^{(n)}, u_{i+1}^{(h)}, p_{i+1}^{(h)}, u_i^{(n)}, p_i^{(n)}, u_i^{(h)}$, and $p_i^{(h)}$. After straightforward algebra manipulations, from Eq. (20) we have

$$\delta V_i^{(n)} = S_i^{(vn)} + f_i^{(pn)}\,\delta p_i^{(n)} + f_i^{(ph)}\,\delta p_i^{(h)}. \qquad (34)$$

Here $S_i^{(vn)}, f_i^{(pn)}$, and $f_i^{(ph)}$ are defined in Eqs. (48), (49) in the Appendix. From Eq. (21), we have

$$\delta u_i^{(n)} = -S_i^{(un)} - a_i^{(un)}\,\delta u_i^{(n)} - a_i^{(uh)}\,\delta u_i^{(h)}. \qquad (35)$$

Here $S_i^{(un)}, a_i^{(un)}$, and $a_i^{(uh)}$ are defined in Eqs. (50), (51) in the Appendix. We write the nonlinear terms at the RHS of Eq. (22) as

$$u_{i+1}^{(h)}p_{i+1}^{(h)} - u_i^{(h)}p_i^{(h)} = u_{i+1}^{(h)}(p_{i+1}^{(h)} - p_i^{(h)}) + p_i^{(h)}(u_{i+1}^{(h)} - u_i^{(h)}),$$

and substitute Eqs. (32), (33) into the equation above for $(p_{i+1}^{(h)} - p_i^{(h)})$ and $(u_{i+1}^{(h)} - u_i^{(h)})$ to have

$$
\begin{aligned}
\delta E_i^{(n)} = &-S_i^{(en)} - b_i^{(un)}\,\delta u_i^{(n)} - b_i^{(uh)}\,\delta u_i^{(h)} \\
&- b_i^{(pn)}\,\delta p_i^{(n)} - b_i^{(ph)}\,\delta p_i^{(h)}.
\end{aligned} \qquad (36)
$$

Here $b_i^{(un)}, b_i^{(uh)}, b_i^{(pn)}$, and $b_i^{(ph)}$ are given in Eqs. (52), (53) in the Appendix, and

$$S_i^{(en)} \equiv u_{i+1}^{(h)}S_i^{(un)} + p_i^{(h)}S_i^{(vn)}. \qquad (37)$$

From Eqs. (34)–(36) and the relation

$$
\begin{aligned}
\delta p_i^{(n)} = &-\rho_i\tilde{p}_i^{(n)}\,\delta V_i^{(n)} - \tfrac{1}{2}(\gamma - 1)\rho_i(\tilde{u}_i^{(n)} + u_i)\,\delta u_i^{(n)} \\
&+ (\gamma - 1)\rho_i\,\delta E_i^{(n)},
\end{aligned}
$$

$\delta p_i^{(n)}$ may be written as

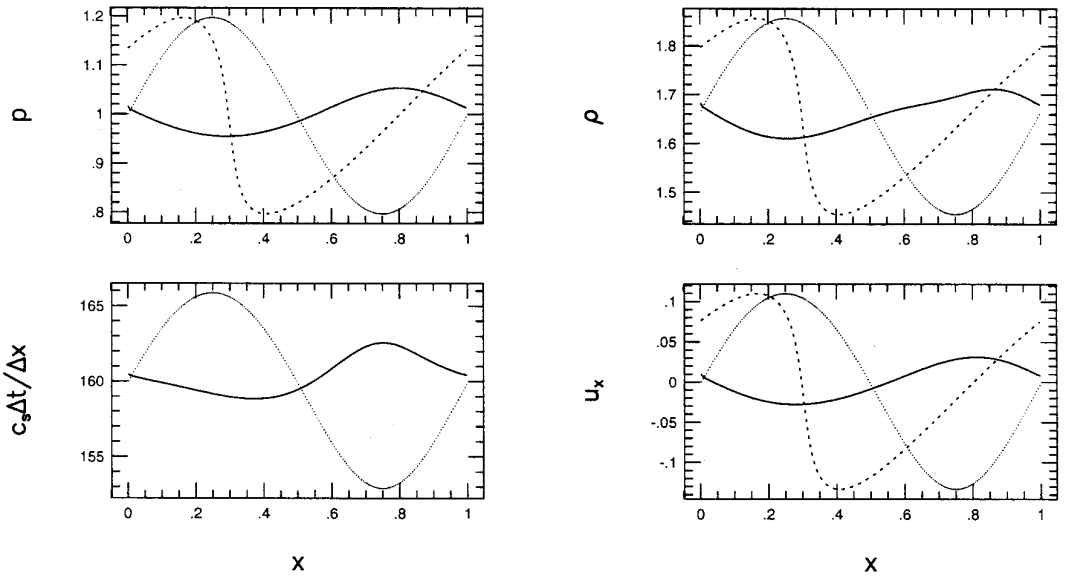

FIG. 10. The sound wave (solid lines) after one time step $\Delta t = 0.8$; 200 cells in [0, 1]; 22 iterations. The initial condition is shown by dotted lines. Dashed lines are from an explicit scheme.

$$\delta p_i^{(n)} = S_i^{(pn)} + d_i^{(un)}\,\delta u_i^{(n)} + d_i^{(uh)}\,\delta u_i^{(h)} + d_i^{(pn)}\delta p_i^{(n)} + d_i^{(ph)}\,\delta p_i^{(h)}. \tag{38}$$

Here $S_i^{(pn)}$, $d_i^{(un)}$, $d_i^{(uh)}$, $d_i^{(pn)}$, and $d_i^{(ph)}$ are defined in Eqs. (54)–(57) in the Appendix.

Similarly, from Eqs. (23)–(25), (30)–(33), we have

$$\delta u_i^{(h)} = -S_i^{(uh)} - \omega_i^{(un)}\,\delta u_i^{(n)} - \omega_i^{(uh)}\,\delta u_i^{(h)}, \tag{39}$$

$$\delta p_i^{(h)} = S_i^{(ph)} + \theta_i^{(un)}\,\delta u_i^{(n)} + \theta_i^{(uh)}\,\delta u_i^{(h)} + \theta_i^{(pn)}\,\delta p_i^{(n)} + \theta_i^{(ph)}\,\delta p_i^{(h)}. \tag{40}$$

Here $S_i^{(uh)}$, $\omega_i^{(un)}$, $\omega_i^{(uh)}$, $S_i^{(ph)}$, $\theta_i^{(un)}$, $\theta_i^{(uh)}$, $\theta_i^{(pn)}$, and $\theta_i^{(ph)}$ are given in Eqs. (58)–(64) in the Appendix.

Finally, we write Eqs. (35), (38)–(40) in the form:

$$-(1 + a_i^{(un)})\,\delta u_i^{(n)} - a_i^{(uh)}\,\delta u_i^{(h)} = S_i^{(un)}, \tag{41}$$

$$-\omega_i^{(un)}\,\delta u_i^{(n)} - (1 + \omega_i^{(uh)})\,\delta u_i^{(h)} = S_i^{(uh)}, \tag{42}$$

$$-d_i^{(un)}\,\delta u_i^{(n)} - d_i^{(uh)}\,\delta u_i^{(h)} + (1 - d_i^{(pn)})\,\delta p_i^{(n)} - d_i^{(ph)}\,\delta p_i^{(h)} = S_i^{(pn)}, \tag{43}$$

$$-\theta_i^{(un)}\,\delta u_i^{(n)} - \theta_i^{(uh)}\,\delta u_i^{(h)} - \theta_i^{(pn)}\,\delta p_i^{(n)} + (1 - \theta_i^{(ph)})\,\delta p_i^{(h)} = S_i^{(ph)}. \tag{44}$$

One iterative procedure for interface values is as follows. Initially, we guess both cell-averages, $\tilde{u}_i^{(h)}$, $\tilde{p}_i^{(h)}$, $\tilde{u}_i^{(n)}$, and $\tilde{p}_i^{(n)}$, and interface values, $u_i^{(h)}$, $p_i^{(h)}$, $u_i^{(n)}$, and $p_i^{(n)}$. Then we improve cell-averages through solving Eqs. (41)–(44) for $\delta u_i^{(n)}$, $\delta u_i^{(h)}$, $\delta p_i^{(n)}$, and $\delta p_i^{(h)}$ with the coefficients and S-terms in Eqs. (41)–(44) evaluated at the initial guess. Thus we are solving two sets of two linear equations. After this, we substitute the improved cell-averages, $\tilde{u}_i^{(h)}$, $\tilde{p}_i^{(h)}$, $\tilde{u}_i^{(n)}$, and $\tilde{p}_i^{(n)}$, into the RHS of Eqs. (30)–(33) to improve interface values, $u_i^{(h)}$, $p_i^{(h)}$, $u_i^{(n)}$, and $p_i^{(n)}$. One iteration consists of the two sets of calculations, one for Eqs. (41)–(44) and the other for Eqs. (30)–(33). The next iteration may be started with the improved cell-averages and interface values if necessary. Numerical experiments show that the iterative procedure converges. We call this iterative approach $\mathbf{A}_1$.

For the calculation of interface values in this implicit–explicit hybrid scheme, a wave propagating in each direction may be either implicitly or explicitly treated depending on the Courant number associated with the wave in each cell. For example, if $c_{si}\Delta t/\Delta x_i$ is less than unity, then $p(x_i^{(m)}, \tau_i\,\Delta t)$ and $u(x_i^{(m)}, \tau_i\,\Delta t)$ in Eqs. (26), (27) are calculated from domain-averages for the wave propagating to the positive x-direction.

3.2. *Multicolors and Convergence of Iterations*

Now we discuss the speed of convergence. We choose a nonlinear wave as an example. The initial wave is set up through differentials of Riemann invariants,

$$\frac{\partial R_+}{\partial x} = 0.4\sin(2\pi x), \tag{45}$$

$$\frac{\partial R_-}{\partial x} = \frac{\partial R_0}{\partial x} = 0, \tag{46}$$

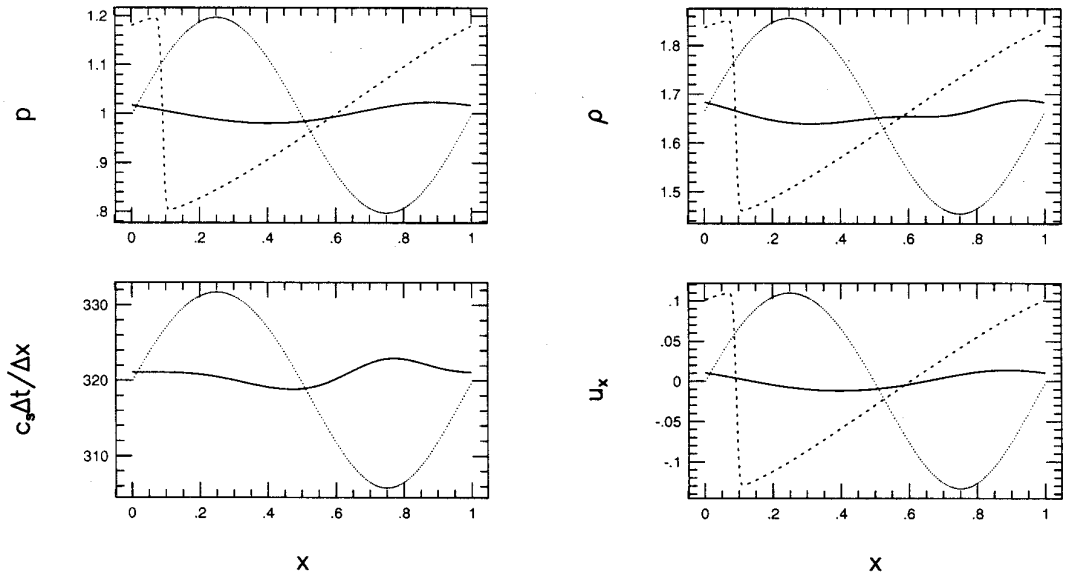

FIG. 11. The sound wave (solid lines) after one time step $\Delta t = 1.6$; 200 cells in [0, 1]; 40 iterations. The initial condition is shown by dotted lines. Dashed lines are from an explicit scheme.

and $\rho(0, 0) = \rho_0$ ($\equiv\frac{5}{3}$) and $p(0, 0) = p_0$ (=1). Here $R_0 \equiv pV^\gamma$. We measure the convergence by the difference between the converged solution and the solution from each iteration:

$$\varepsilon_{1d} = \frac{1}{L}\sum_{i=1}^{N}\Delta x_i^{(n)}\left[\frac{1}{p_0}\left|p_i^{(n)} - p_{i,*}^{(n)}\right| + \frac{1}{c_0}\left|u_i^{(n)} - u_{i,*}^{(n)}\right|\right] + \frac{1}{L}\sum_{i=1}^{N}\Delta x_i^{(h)}\left[\frac{1}{p_0}\left|p_i^{(h)} - p_{i,*}^{(h)}\right| + \frac{1}{c_0}\left|u_i^{(h)} - u_{i,*}^{(h)}\right|\right].$$

Here L (=1) is the wavelength, the subscript $*$ stands for the converged solution, and $\Delta x_i^{(n)}$ and $\Delta x_i^{(h)}$ are the widths of the ith cell in the Lagrangian coordinate at $t = \Delta t$ and $\Delta t/2$. Figure 3 shows the convergence when a uniform grid with $N = 200$ cells in a wavelength and a time step 0.2 are used. $c_{si}\,\Delta t/\Delta x_i \approx 40$. The dotted line in Fig. 3 shows the relation between ε_{1d} and the number of iterations obtained from the approach $\mathbf{A}_1$. Many iterations are needed for a reasonably accurate interface values (e.g., $\varepsilon_{1d} = 10^{-5}$), since information travels only one numerical cell through each iteration in the approach $\mathbf{A}_1$.

To improve the speed of convergence, we divide all numerical cells into two sets: $\{i;\, i = 2j + 1,\, j = 0, 1, 2, ...\}$ and $\{i;\, i = 2j,\, j = 1, 2, ...\}$, which are called red and black sets. Equations (41)–(44) are first implemented for the red set of cells followed by an evaluation of the S-terms in Eqs. (41)–(44), and then Eqs. (41)–(44) are implemented for the other set of cells. This approach converges more rapidly than $\mathbf{A}_1$ since information travels two cells through each iteration. We call the approach $\mathbf{A}_2$. The result obtained from $\mathbf{A}_2$ is shown by the solid line indicated by $k = 2$ in Fig. 3.

To further develop the strategy, we divide all numerical cells into k (>2) groups $\mathbf{G}_l$ ($l = 1, 2, ..., k$), i.e., k different colors, and the lth group contains cells $\{i;\, i = (j - 1)k + l,\, j = 1, 2, ...\}$. For example, when $k = 4$, the four groups $\mathbf{G}_l$ ($l = 1, 2, 3, 4$) are $\{i = 1, 5, 9, ...\}$, $\{i = 2, 6, 10, ...\}$, $\{i = 3, 7, 11, ...\}$, and $\{i = 4, 8, 12, ...\}$. An iteration consists of the implementation of Eqs. (41)–(44) for groups $\mathbf{G}_1$, $\mathbf{G}_2$, ..., $\mathbf{G}_k$ (or $\mathbf{G}_k$, $\mathbf{G}_{k-1}$, ..., $\mathbf{G}_1$) followed by another iteration with the opposite order, i.e., from $\mathbf{G}_k$ to $\mathbf{G}_1$ (or from $\mathbf{G}_1$ to $\mathbf{G}_k$). We call the approach $\mathbf{A}_k$. Results obtained from $\mathbf{A}_6$, $\mathbf{A}_{10}$, $\mathbf{A}_{20}$, $\mathbf{A}_{50}$, and $\mathbf{A}_{100}$ are given by the solid lines indicated by $k = 6$, 10, 20, 50, and 100 in Fig. 3. Generally, an approach $\mathbf{A}_k$ with a larger k will result in a faster convergence since information may travel k cells through each iteration in the approach $\mathbf{A}_k$. We have to mention that since information is carried by sound waves propagating in two directions, the change in the order to implement Eqs. (41)–(44) for groups $\mathbf{G}_l$ ($l = 1, 2, ..., k$) is necessary for the improvement.

The advantage of the implicit–explicit scheme becomes more obvious if it is used in a very fine mesh. Figure 4 shows the convergence when a uniform grid with $N = 2000$ in a wavelength and a time step 0.2 are used. Courant numbers are around 400, and the wave travels about one-fifth of its wavelength during the time step. The number of iterations required to reach a converged solution is reduced by several orders by the introduction of the multicolors.

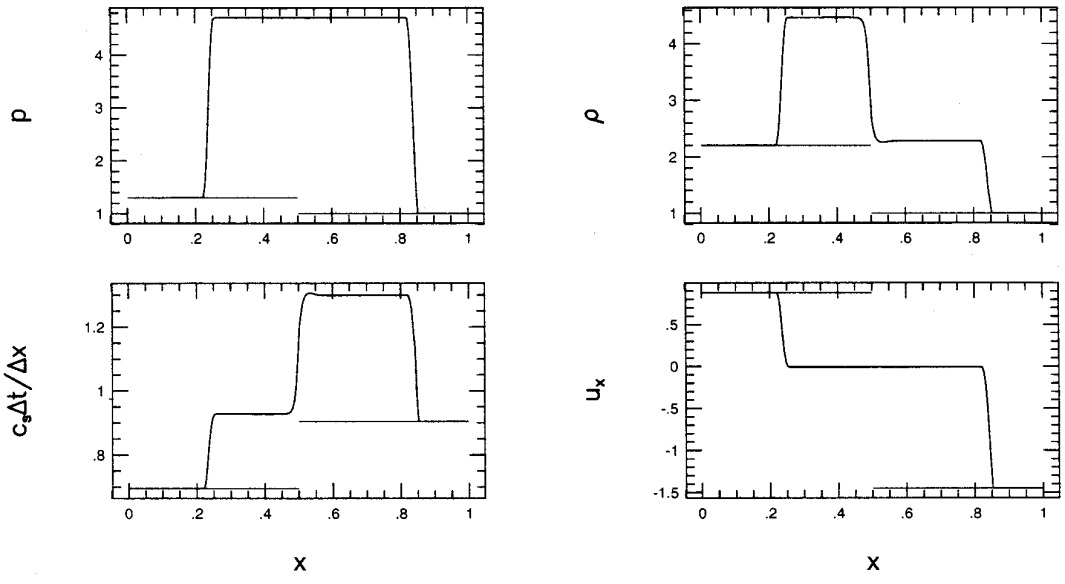

FIG. 12. A shock-tube problem: $\Delta t = 0.0035$; 200 cells in [0, 1]; 5 iterations. Initially, (ρ, p, u_x) is equal to $(1, 1, -1.45)$ for $x > 0.5$ and is equal to (2.2, 1.3, 0.88) for $x < 0.5$, as shown by dotted lines. Solid lines are the profiles at $t = 0.3$, which contain two shocks and a contact discontinuity.

There are two points we would like to mention here. First, we do not have to find converged interface values in the scheme. Only approximate interface values are needed in Eqs. (20)–(22). The number of iterations used in the numerical examples to be presented in the paper only guarantees the error ε_{1d} less than 10^{-4}. After we find the approximate solutions for interface values, we use Eqs. (20)–(22) to update conserved quantities. Therefore, the mass, momentum, and energy are exactly conserved in the scheme. Second, the coefficients in Eqs. (41)–(44) are evaluated only once in each iteration. Thus the use of the multicolors does not involve more calculations than a single color.

3.3. *Mapping from Lagrangian to Eulerian Grids*

The values of conserved quantities in the original Eulerian grid are obtained through mapping from the Lagrangian grid to the Eulerian grid. The mapping is only a transformation between two grids. In the mapping, the mass, momentum, and energy should be conserved. Consider the Lagrangian and Eulerian grids denoted by $\{x_i^{(l)}\}$ and $\{x_i\}$, respectively. For the mapping, we have to find the intergral of $a(x)$ over the cell $[x_i, x_{i+1}]$ of the Eulerian grid. The cell-average of a over the cell is the integral divided by the cell width. Note that a cell in the Eulerian grid, $[x_i, x_{i+1}]$, may extend over several cells in the Lagrangian grid. The contribution of a cell in the Lagrangian grid, which is completely overlapped by the domain $[x_i, x_{i+1}]$, to the integral is simply the cell-average multiplied by the width of the cell. For those cells in the Lagrangian grid which are partially overlapped by the domain $[x_i, x_{i+1}]$, we have to find the integral of $a(x)$ over the domain $[s_0, s_1]$ which is a part of a cell $[x_j^{(l)}, x_{j+1}^{(l)}]$, as shown in Fig. 5. Cubic polynomials are used to interpolate a conserved quantity a in order to find values at interfaces of numerical cells in the Lagrangian grid. From a parabolic interpolation uniquely determined by the cell-average a_j and values at the left and right interfaces, a_l and a_r, the integral is found to be

$$\int_{s_0}^{s_1} a(x)\,dx = (s_1 - s_0)\left[a_l + \frac{1}{2}(\hat{a}_j + a_r - a_l)(\xi_j + \zeta_j) - \frac{1}{3}\hat{a}_j(\xi_j^2 + \xi_j\zeta_j + \zeta_j^2)\right]. \tag{47}$$

Here

$$\xi_j \equiv \frac{s_1 - x_j^{(l)}}{x_{j+1}^{(l)} - x_j^{(l)}}, \quad \zeta_j \equiv \frac{s_0 - x_j^{(l)}}{x_{j+1}^{(l)} - x_j^{(l)}},$$
$$\hat{a}_j \equiv 6a_j - 3(a_l + a_r).$$

In the mapping, either s_1 or s_0 is an interface of cells.

4. NUMERICAL EXAMPLES

The scheme has been tested for numerical examples, some of which will be presented here to illustrate the properties of the scheme. Calculations with different numbers of colors may result in equally accurate interface values. Therefore, solutions from simulations with different numbers of colors are the same. Here we present only the

results from the approach $\mathbf{A}_{50}$. The value for γ is set to $\frac{5}{3}$. A uniform grid with 200 cells is used. Calculations are performed for different time steps which show how the scheme treats waves with different wavelengths.

The first example is the propagation of a sound wave initially determined by Eqs. (45), (46) with a shifted flow velocity u_x. The initial condition is shown by the dotted lines in Fig. 6. The time step is 0.005. At each time step, the sound wave is partially implicitly and partially explicitly calculated. The solid lines in Fig. 6 are the profiles at $t =$ 0.5, 1.0, 1.5, and 2.0. The results show a smooth switch between explicit and implicit calculations.

Figs. 7–11 show the profiles of the wave after one time step when different time steps are used. The dashed lines in Figs. 7–11 are references obtained from an explicit scheme (the PPM) with Courant numbers around 0.8. As shown in Fig. 7, when $c_s\ \Delta t/\Delta x \approx 20$, it is hard to see the difference between the implicit and explicit schemes. Figure 8 shows the difference when the time step is increased to $\Delta t \approx 40\ \Delta x/c_s$. The wave is significantly damped in Fig. 9 when the time step is increased to $\Delta t \approx 80\ \Delta x/c_s$. If Courant numbers are larger than the number of numerical cells in one wavelength, the profiles after one time step are close to constant states. If the time step is very large, an approximately steady state may be reached.

5. CONCLUSIONS AND DISCUSSIONS

We have developed an iterative approach for the implicit–explicit hybrid scheme proposed by Fryxell *et al.* [15] for the one-dimensional Euler equations. The scheme is of Godunov-type, is in a strictly conservative form, is accurate to second order in both space and time for all Courant numbers, is able to smoothly switch between implicit and explicit calculations, and keeps the advantages of Godunov schemes. The scheme has advantages for those problems in which the time accuracy is important at least in some part of a simulation domain.

The iterative approach proposed in this paper involves only a single level of iterations, which solve both the implicit relations arising from upstream centered differences for all wave families and the nonlinearity of the Euler equations. Compared with large Courant numbers in a simulation with large time steps, only a small number of iterations are needed for the flux calculation in the scheme. The multicolors proposed in this paper further develop the red–black strategy. Information travels two cells through each iteration in the red–black approach. Information may travel k cells through one iteration in the approach $\mathbf{A}_k$ proposed in this paper, where k may be any reasonable number between 2 and the number of cells. The number of iterations required to reach a converged solution may be significantly reduced through the introduction of the multicolors. The multicolors may also be applied to other linear and nonlinear wave equations for numerical solutions.

Finally, we would like to discuss shock-tube problems and performance of the scheme. We do not recommend the use of an implicit scheme for shock-tube problems. If discontinuities have to be resolved in some part of a simulation domain, sizes of time steps should be restricted so that Courant numbers remain around or less than unity in that part of the domain. Figure 12 shows a solution obtained from the implicit–explicit hybrid scheme for a shock tube problem which involves two shocks and a contact discontinuity. Our current computer code for the scheme shows that the computations needed for each iteration in one time step are about 50% of those needed in one time step of an equivalent explicit scheme, such as PPM. Thus the computations needed for one time step of the hybrid scheme with 10 iterations are about six times of the computations needed in one time step of the explicit scheme, and the computations needed in one time step of the hybrid scheme with 20 iterations are about 11 times of the computations needed in one time step of the explicit scheme.

APPENDIX

In this appendix, we list some definitions used in this paper. $S_i^{(vn)}$, $f_i^{(pn)}$ and $f_i^{(ph)}$ in Eq. (35) are defined as

$$\begin{aligned} S_i^{(vn)} \equiv & \frac{\Delta t}{2\,\Delta m_i}\left[\tilde{u}_{i+1} - u_{i-1} - \frac{1}{w_{i+1}}(p_{i+1} - p_i) + \frac{1}{w_i}(p_i - p_{i-1})\right] \\ & - \frac{\Delta t}{2\,\Delta m_i}\left[\alpha_{i-1}^{(h)}\,\delta u_{i-1}^{(n)} + \beta_{i-1}^{(h)}\,\delta u_{i-1}^{(h)} + \frac{1}{w_i}(\alpha_{i-1}^{(h)}\,\delta p_{i-1}^{(n)} + \beta_{i-1}^{(h)}\,\delta p_{i-1}^{(h)}\right] \\ & + \frac{\Delta t}{2\,\Delta m_i}\alpha_{i+1}^{(h)}\,\delta u_{i+1}^{(n)} + \beta_{i+1}^{(h)}\,\delta u_{i+1}^{(h)} - \frac{1}{w_{i+1}}(\alpha_{i+1}^{(h)}\,\delta p_{i+1}^{(n)} + \beta_{i+1}^{(h)}\,\delta p_{i+1}^{(h)})\Bigg], \end{aligned} \tag{48}$$

$$f_{i-1}^{(pn)} \equiv \frac{\Delta t}{2\,\Delta m_i}\alpha_i^{(h)}\left(\frac{1}{w_{i+1}} + \frac{1}{w_i}\right),$$

$$f_i^{(ph)} \equiv \frac{\Delta t}{2\,\Delta m_i}\beta_i^{(h)}\left(\frac{1}{w_{i+1}} + \frac{1}{w_i}\right). \tag{49}$$

$S_i^{(un)}$, $a_i^{(un)}$, and $a_i^{(uh)}$ in Eq. (35) are defined as

$$S_i^{(un)} \equiv \frac{\Delta t}{2\,\Delta m_i}[p_{i+1} - p_{i-1} + w_i(u_i - u_{i-1}) - w_{i+1}(u_{i+1} - u_i)] - \frac{\Delta t}{2\,\Delta m_i}[\alpha_{i-1}^{(h)}\,\delta p_{i-1}^{(n)} + \beta_{i-1}^{(h)}\,\delta p_{i-1}^{(h)} + w_i(\alpha_{i-1}^{(h)}\,\delta u_{i-1}^{(n)} + \beta_{i-1}^{(h)}\,\delta u_{i-1}^{(h)})] + \frac{\Delta t}{2\,\Delta m_i}[\alpha_{i+1}^{(h)}\,\delta p_{i+1}^{(n)} + \beta_{i+1}^{(h)}\,\delta p_{i+1}^{(h)} - w_{i+1}(\alpha_{i+1}^{(h)}\,\delta u_{i+1}^{(n)} + \beta_{i+1}^{(h)}\,\delta u_{i+1}^{(h)})], \tag{50}$$

$$a_i^{(un)} \equiv \frac{\Delta t}{2\,\Delta m_i}\alpha_i^{(h)}(w_i + w_{i+1}),$$

$$a_i^{(uh)} \equiv \frac{\Delta t}{2\,\Delta m_i}\beta_i^{(h)}(w_i + w_{i+1}). \tag{51}$$

$b_i^{(un)}, b_i^{(uh)}, b_i^{(pn)}$, and $b_i^{(ph)}$ in Eq. (36) are defined as

$$b_i^{(un)} \equiv u_{i+1}^{(h)} a_i^{(un)}, \quad b_i^{(uh)} \equiv u_{i+1}^{(h)} a_i^{(uh)}, \tag{52}$$

$$b_i^{(pn)} \equiv p_i^{(h)} f_i^{(pn)}, \quad b_i^{(ph)} \equiv p_i^{(h)} f_i^{(ph)}, \tag{53}$$

$S_i^{(pn)}, d_i^{(un)}, d_i^{(uh)}, d_i^{(pn)}$, and $d_i^{(ph)}$ in Eq. (38) are defined as

$$S_i^{(pn)} \equiv -\rho_i \tilde{p}_i^{(n)} S_i^{(vn)} + \tfrac{1}{2}(\gamma - 1)\,\rho_i(\tilde{u}_i^{(n)} + u_i) S_i^{(un)} \tag{54}$$

$$- (\gamma - 1)\rho_i S_i^{(en)}, \tag{55}$$

$$d_i^{(un)} \equiv \tfrac{1}{2}(\gamma - 1)\rho_i(\tilde{u}_i^{(n)} + u_i)a_i^{(un)} - (\gamma - 1)\rho_i b_i^{(un)}, \tag{56}$$

$$d_i^{(uh)} \equiv \tfrac{1}{2}(\gamma - 1)\rho_i(\tilde{u}_i^{(n)} + u_i)a_i^{(uh)} - (\gamma - 1)\rho_i b_i^{(uh)},$$

$$d_i^{(pn)} \equiv -\rho_i \tilde{p}_i^{(n)} f_i^{(pn)} - (\gamma - 1)\rho_i b_i^{(pn)},$$

$$d_i^{(ph)} \equiv -\rho_i \tilde{p}_i^{(n)} f_i^{(ph)} - (\gamma - 1)\rho_i b_i^{(ph)}. \tag{57}$$

$S_i^{(uh)}$, $\omega_i^{(un)}$, and $\omega_i^{(uh)}$ in Eq. (39) are defined as

$$S_i^{(uh)} \equiv \frac{\Delta t}{2\,\Delta m_i}\left[\frac{1}{2}(p_{i+1} - p_{i-1}) + \frac{1}{4}(u_i - u_{i-1})(3w_i - w_i^{(h)}) - \frac{1}{4}(u_{i+1} - u_i)(3w_{i+1} - w_{i+1}^{(h)})\right] + \frac{\Delta t}{2\,\Delta m_i}[g_{i+1}^{(un)}\,\delta p_{i+1}^{(n)} + g_{i+1}^{(uh)}\,\delta p_{i+1}^{(h)} + q_{i+1}^{(un)}\,\delta u_{i+1}^{(n)} + q_{i+1}^{(uh)}\,\delta u_{i+1}^{(h)}] - \frac{\Delta t}{2\,\Delta m_i}[g_{i-1}^{(un)}\,\delta p_{i-1}^{(n)} + g_{i-1}^{(uh)}\,\delta p_{i-1}^{(h)} + \nu_{i-1}^{(un)}\,\delta u_{i-1}^{(n)} + \nu_{i-1}^{(uh)}\,\delta u_{i-1}^{(h)}], \tag{58}$$

$$\omega_i^{(un)} \equiv \frac{\Delta t}{2\,\Delta m_i}(\nu_i^{(un)} - q_i^{(un)}), \quad \omega_i^{(uh)} \equiv \frac{\Delta t}{2\,\Delta m_i}(\nu_i^{(uh)} - q_i^{(uh)}). \tag{59}$$

Here

$$g_i^{(un)} \equiv \tfrac{1}{4}(3\alpha_i^{(h)} - \alpha_i^{(n)}), \qquad g_i^{(uh)} \equiv \tfrac{1}{4}(3\beta_i^{h)} - \beta_i^{(n)}),$$

$$q_i^{(un)} \equiv \tfrac{1}{4}(w_i^{(h)}\,\alpha_i^{(n)} - 3w_i\alpha_i^{(h)}), \quad q_i^{(uh)} \equiv \tfrac{1}{4}(w_i^{(h)}\beta_i^{(n)} - 3w_i\beta_i^{(h)}),$$

$$\nu_i^{(un)} \equiv \tfrac{1}{4}(3w_{i+1}\alpha_i^{(h)} - w_{i+1}^{(h)}\alpha_i^{(n)}, \quad \nu_i^{(uh)} \equiv \tfrac{1}{4}(3w_{i+1}\beta_i^{(h)} - w_{i+1}^{(h)}\beta_i^{(n)}).$$

$S_i^{(ph)}$, $\theta_i^{(un)}$, $\theta_i^{(uh)}$, $\theta_i^{(pn)}$, and $\theta_i^{(ph)}$ in Eq. (40) are defined as

$$S_i^{(ph)} \equiv -\rho_i \tilde{p}_i^{(h)} S_i^{(vh)} + \tfrac{1}{2}\rho_i(\tilde{u}_i^{(h)} + \tilde{u}_i) S_i^{(uh)} - (\gamma - 1)\rho_i S_i^{(eh)}, \tag{60}$$

$$\theta_i^{(un)} \equiv \tfrac{1}{2}(\gamma - 1)\rho_i(\tilde{u}_i^{(h)} + u_i)\omega_i^{(un)} - (\gamma - 1)\rho_i \eta_i^{(un)}, \tag{61}$$

$$\theta_i^{(uh)} \equiv \tfrac{1}{2}(\gamma - 1)\rho_i(\tilde{u}_i^{(h)} + u_i)\omega_i^{(uh)} - (\gamma - 1)\rho_i \eta_i^{(uh)}, \tag{62}$$

$$\theta_i^{(pn)} \equiv -\frac{\Delta t}{2\,\Delta m_i}\rho_i \tilde{p}_i^{(h)}(\mu_i^{(pn)} - g_i^{(pn)}) - (\gamma - 1)\rho_i \eta_i^{(pn)}, \tag{63}$$

$$\theta_i^{(ph)} \equiv -\frac{\Delta t}{2\,\Delta m_i}\rho_i \tilde{p}_i^{(h)}(\mu_i^{(ph)} - g_i^{(ph)}) - (\gamma - 1)\rho_i \eta_i^{(ph)}, \tag{64}$$

Here

$$S_i^{(vh)} \equiv \frac{\Delta t}{2\,\Delta m_i}\left[\frac{1}{2}(u_{i+1} - u_{i-1}) + \frac{1}{4}(p_i - p_{i-1})\left(\frac{3}{w_i} - \frac{1}{w_i^{(h)}}\right) - \frac{1}{4}(p_{i+1} - p_i)\left(\frac{3}{w_{i+1}} - \frac{1}{w_{i+1}^{(h)}}\right)\right] + \frac{\Delta t}{2\,\Delta m_i}[g_{i+1}^{(un)}\,\delta u_{i+1}^{(n)} + g_{i+1}^{(uh)}\,\delta u_{i+1}^{(h)} + g_{i+1}^{(pn)}\,\delta p_{i+1}^{(n)} + g_{i+1}^{(ph)}\,\delta p_{i+1}^{(h)}] - \frac{\Delta t}{2\,\Delta m_i}[g_{i-1}^{(un)}\,\delta u_{i-1}^{(n)} + g_{i-1}^{(uh)}\,\delta u_{i-1}^{(h)} + \mu_{i-1}^{(pn)}\,\delta p_{i-1}^{(n)} + \mu_{i-1}^{(ph)}\,\delta p_{i-1}^{(h)}],$$

$$S_i^{(eh)} \equiv \left(\frac{3}{2}p_{i+1}^{(h)} - \frac{1}{2}p_{i+1}^{(n)}\right) S_i^{(vh)} + \left(\frac{3}{2}u_i^{(h)} - \frac{1}{2}u_i^{(n)}\right) S_i^{(uh)}$$

$$g_i^{(pn)} \equiv \frac{1}{4}\left(\frac{\alpha_i^{(n)}}{w_i^{(h)}} - \frac{3\alpha_i^{(h)}}{w_i}\right), \quad g_i^{(ph)} \equiv \frac{1}{4}\left(\frac{\beta_i^{(n)}}{w_i^{(h)}} - \frac{3\beta_i^{(h)}}{w_i}\right),$$

$$\mu_i^{(pn)} \equiv \frac{1}{4}\left(\frac{3\alpha_i^{(h)}}{w_{i+1}} - \frac{\alpha_i^{(n)}}{w_{i+1}^{(h)}}\right), \quad \mu_i^{(ph)} \equiv \frac{1}{4}\left(\frac{3\beta_i^{(h)}}{w_{i+1}} - \frac{\beta_i^{(n)}}{w_{i+1}^{(h)}}\right),$$

$$\eta_i^{(un)} \equiv \left(\frac{3}{2}u_i^{(h)} - \frac{1}{2}u_i^{(n)}\right)\omega_i^{(un)},$$

$$\eta_i^{(uh)} \equiv \left(\frac{3}{2}u_i^{(h)} - \frac{1}{2}u_i^{(n)}\right)\omega_i^{(uh)},$$

$$\eta_i^{(pn)} \equiv \frac{\Delta t}{2\,\Delta m_i}\,(\mu_i^{(pn)} - g_i^{(pn)})\left(\frac{3}{2}p_{i+1}^{(h)} - \frac{1}{2}p_{i+1}^{(n)}\right),$$

$$\eta_i^{(ph)} \equiv \frac{\Delta t}{2\,\Delta m_i}\,(\mu_i^{(ph)} - g_i^{(ph)})\left(\frac{3}{2}p_{i+1}^{(h)} - \frac{1}{2}p_{i+1}^{(n)}\right).$$

ACKNOWLEDGMENTS

The authors wish to thank B. Fyxell, and Wenlong Dai wishes to thank H. Chen, for the discussion about implicit schemes. This work was supported by the U.S. National Science Foundation under Grant NSF-ASC-9309829, by the Minnesota Supercomputer Institute, and by the Army Research Office contract number DAALO3-89-C-0038 with Army High Performance Computing Research Center at the University of Minnesota.

REFERENCES

1. S. K. Godunov, *Math. Sb.* **47,** 271 (1959).
2. B. Van Leer, *J. Comput. Phys.* **23,** 276 (1977).
3. B. Van Leer, *J. Comput. Phys.* **32,** 101 (1979).
4. P. L. Roe, *J. Comput. Phys.* **43,** 358 (1981).
5. P. R. Woodward and P. Colella, *Lecture Notes in Physics,* Vol. **141** (Springer-Verlag, New York/Berlin, (1981), p. 434.
6. P. Colella and P. R. Woodward, *J. Comput. Phys.* **54,** 174 (1984).
7. A. Harten, *J. Comput. Phys.* **49,** 359 (1983).
8. H. B. Keller and P. R. Wendroff, *Comm. Pure Appl. Math.* **10,** 567 (1957).
9. S. Nakamura, *Computational Method in Engineering and Science* (Wiley, New York, 1976), p. 175.
10. R. W. Beam and R. F. Warming, *J. Comput. Phys.* **22,** 87 (1976).
11. B. Engquist and S. Osher, *Math. Comput.* **34,** 45 (1980).
12. B. Van Leer and W. A. Mulder, in *Numerical methods for the Euler Equations of Fluid Dynamics*, edited by F. Angrand, A. Dervieux, J. A. Desideri, and R. Glowinski (SIAM, Philadelphia, 1985), p. 312.
13. H. C. Yee, R. F. Warming, and A. Harten, *J. Comput. Phys.* **57,** 327 (1985).
14. H. M. Glaz and A. B. Wardlaw, *J. Comput. Phys.* **58,** 157 (1985); **12A,** 413 (1986).
15. B. A. Fryxell, P. R. Woodward, P. Colella, and K.-H. Winkler, *J. Comput. Phys.* **63,** 283 (1986).
16. A. Jameson and S. Yoon, *AIAA J.* **24,** 1737 (1986).
17. A. Jameson and S. Yoon, *AIAA J.* **25,** 929 (1987).
18. C. Y. Loh and W. H. Hui, *J. Comput. Phys.* **89,** 207 (1990).
19. M. Blunt and B. Rubin, *J. Comput. Phys.* **92,** 194 (1992).
20. M. Wilcoxson and V. Manousiouthakis, *J. Comput. Phys.* **115,** 376 (1994).